

SOGHAN COMPLEX AS AN EVIDENCE FOR PALEOSPREADING CENTER AND MANTLE DIAPIRISM IN SANANDAJ-SIRJAN ZONE (SOUTH-EAST IRAN)

H. Ahmadipour^{1,*}, M. Sabzehei², H. Whitechurch³, E. Rastad⁴, and M.H. Emami²

¹ *Department of Geology, Faculty of Sciences, Shahid Bahonar University of Kerman,
P.O. Box 133-76135, Kerman, Islamic Republic of Iran*

² *Institute for Earth Sciences Research, Geological Survey of Iran, Tehran, Islamic Republic of Iran*

³ *University of Louis Pasteur, Strasburg, France*

⁴ *Department of Geology, Faculty of Sciences, Tarbiat Modarres University, Tehran, Islamic Republic of Iran*

Abstract

Soghan complex is one of the major ultramafic-mafic complexes in south-east Iran (Esfandagheh area). Lower part of this complex is composed of dunite, harzburgite and chromitite. The lower part is transitionally converted to lherzite, dunite, pyroxenite and wehrlite (transition zone). These units are transitionally changed into layered gabbros. This sequence is overlain by the metamorphosed Sargaz-Abshur complexes (Marble and Amphibolites) and has been invaded by an isotropic gabbro in Upper Triassic-lower Jurassic period. The last magmatic phase in this complex is characterised by Cretaceous diabasic dykes. Dunites and harzburgites have coarse granular texture with evidence of grain boundary migration and annealing. In these rocks, there are two generations of minerals; the first generation is completely deformed but the second one is nondeformed which have been probably recrystallized from ascending melts. Soghan peridotites have a weak lattice preferred orientation similar to the mantle peridotites. Layered gabbros have typical cumulate textures and phase layering. There are various shapes of minerals with different chemical composition in Soghan complex. The whole chemical composition of Soghan chromitites in particular TiO₂ and Cr₂O₃ contents are similar to boninitic chromites. However, disseminated chromspinel of harzburgites plot in the field of refractory depleted chromspinel. Geothermometric estimations on orthopyroxene-clinopyroxene and olivine-spinel in the complex show subsolidus equilibrium temperatures ranging from 800-950°C. Based on the petro-geochemical data, Soghan harzburgites have been formed by partial melting of subcontinental lherzolites with minor percolation of later melts. The absence of pillow lavas and tectonites, combined with textures, mineral chemistry and whole rock chemistry indicate this complex is likely a part of mantle diapir. Paleorifting of aborted types in Paleozoic, caused lherzolitic diapirism in this area. At the first stage, the diapir is partially melted and resulting melts form transition zone and layered gabbros. In later stages of partial melting, ultramafic sills and isotropic gabbro were formed and move upward. These could have reacted with host peridotites and formed chromite bearing dunites. It is probable that in early Kimmerian orogenic phase, the whole sequence was metamorphosed up to amphibolite facies.

Keywords: Ultramafic-mafic complexes; Chromitite; Diapirism

1. Introduction

Soghan ultramafic-mafic complex is located in south-

east of Iran, extremity of Sanandaj-Sirjan metamorphic zone in the Esfandagheh area (south of Kerman province) (Fig. 1). This area is located in a very

* E-mail: hahmadi@mail.uk.ac.ir

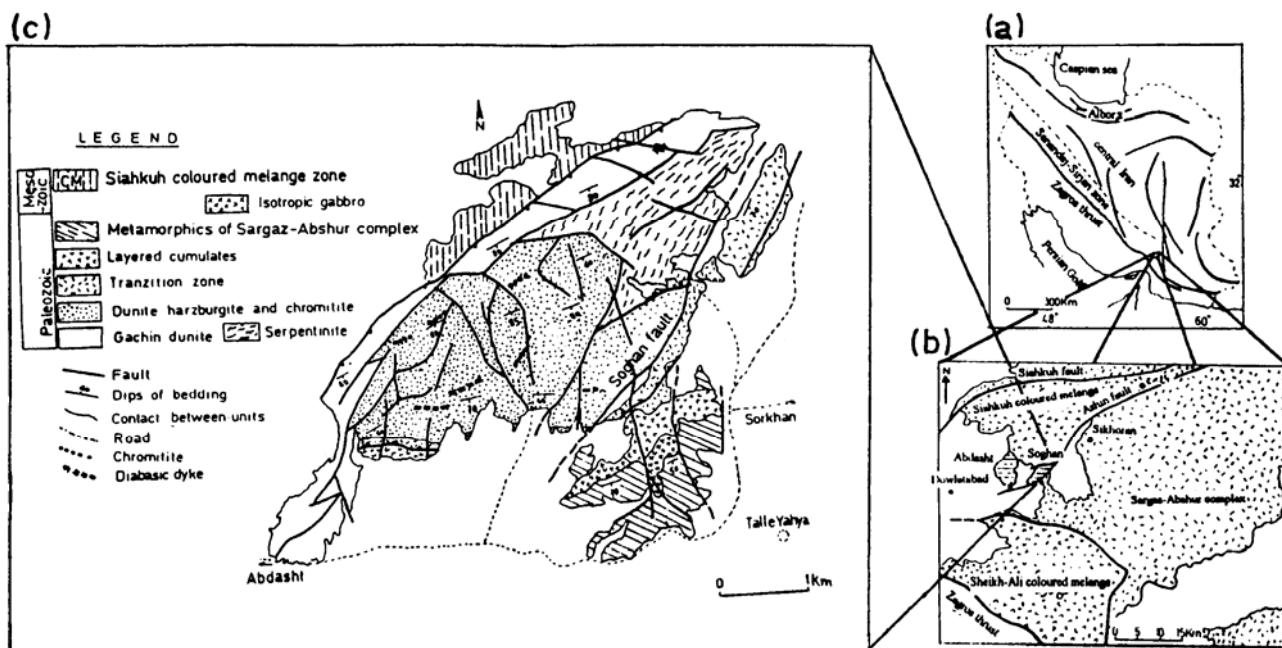


Figure 1. a) Situation of Esfandagheh region in Iran [29], b) Situation of Soghan, Abdasht, Sikhoran and Sharikabad massives in Esfandagheh region, c) Geological map of Soghan massif [1].

tectonically active zone, materialized by highly deformed metamorphic rocks, coloured melange and ultramafic-mafic complexes.

Sabzehei [29] considered this geological unit as a part of Sanandaj-Sirjan Zone and believed that Soghan complex has been initiated from differentiation of a tholeiitic magma similar to those of Esfandagheh ultramafic associations. Stocklin [33] assumed ultramafic associations of this area belong to Rezaieh-Esfandagheh ophiolites. Detailed map of Soghan complex (scale 1:5000) for chromite exploration [31] characterized the complex as ultramafic layered complex of Lower Paleozoic-Upper Precambrian age. Sabzehei [31] believes that these complexes are formed from differentiation of a huge mass of ultramafic magma in Upper Proterozoic-Lower Paleozoic in an intracontinental rift basin.

The aim of this paper is to show some evidences of extensional tectonic and mantle diapirism in this region and describe precisely geological setting showing the first results of dating, structural and geochemical data in order to find the geological evolution of Soghan complex. Ahmadipour [2] studied this complex comprehensively and suggested model of diapirism.

This paper for the first time introduces petrographical, mineralogical and geochemical data for presenting a possible model of diapirism for the structural evolution of the area.

2. Sampling, Methodology and Analytical Methods

Systematic sampling was done by Ahmadipour in 1999 [2] from all units. Samples were crushed and milled in Tarbiat Modarres University (Tehran). The system was free of possible contamination. The samples were sent to the geochemical and age dating laboratories for the following analyses:

a) Age dating analyses that have been made by K-Ar method on the amphibole and whole rock (6 analyses) in age dating laboratory of Louis Pasteur University.

b) For the mineral chemistry, several minerals (more than 800 points in 100 thin sections) have been analysed by a CAMEBAX SX50 microprobe (Jusieu, and Bertagne Occidentale, France). The accelerating voltage was 15 kV. The beam current was 12 nA with the counting time varying from 10-20 s.

c) Whole rock analysis on the Soghan samples have made by ICP-ES in the University of Bertagne Occidentale (Brest) and ICP-MS in the Louis Pasteur University (77 analyses).

3. Geological Setting

The Soghan complex is located in the south-east of Sanandaj-Sirjan metamorphic zone (Esfandagheh area) (Fig. 1). In the Esfandagheh area there are several

igneous, sedimentary and metamorphic units, that are:

a) Ultramafic-mafic complexes of Soghan, Abdasht and Sikhoran.

b) Sargaz-Abshur metamorphic complexes or Paleozoic metamorphites of Sanandaj-Sirjan Zone. Abshur complex contains alternative marble, amphibolite and minor micaschist of Paleozoic age [29]. Sargaz complex is composed of greenschist, minor marble, quartzite and micaschist (Fig. 1).

c) A sedimentary-igneous association of Jurassic-Cretaceous. This complex overlies the Sargaz-Abshur complexes with an angular unconformity and contains flysch, turbidites and calpionella limestone.

d) Coloured melange zones such as Siah kuh and south Dowlatabad melanges.

e) Granitoid intrusive bodies.

Other layered ultramafic-mafic complexes such as Abdasht and Sikhoran show similar petrological features.

On the north of Soghan complex, a coloured melange zone has been mapped by Sabzehei *et al.* [30] which includes glaucophane schist, serpentinite, flysch type sediments, pillow lava and pelagic limestone, separated by a reverse fault (N 60/80 SE) from Soghan complex.

4. Lithological and Petrographical Descriptions of the Soghan Complex

Soghan complex is composed of five main units: The Gachin unit, the main Soghan unit, the transition zone and layered gabbros overlain by Sargaz-Abshur metamorphic unit. All of these units have been invaded by an isotropic gabbro (Fig. 1). These units from below to top are as followings:

4.1. Gachin Peridotites

This unit is located in the northern border of the Soghan complex with faulted contact either with coloured melange zone or other units of the complex (Fig. 1). It is composed of strongly serpentinized dunite, harzburgite and minor chromitite, has a weakly layering structure disturbed by many faults. They are strongly deformed and have mechanical twinning and granular texture. Fibrous serpentine has grown between them and implies that serpentinization is dynamic and deformation is cold. They are strongly deformed and have mechanical twinning and granular texture. Orthopyroxenes are strongly altered into serpentine, amphiboles and opaque minerals. They are completely deformed and have sigmoidal shape and one can recognize them by their relicts. Chromospinel occurs as disseminated medium grain size (up to 2 mm) in

harzburgites. Clinopyroxene usually has altered to tremolitic and actinolitic hornblende. Dunites, in this unit, are almost completely altered to serpentine. In some exposures there are chromitite massive ores (Gachin mine).

4.2. The Main Soghan Unit

This unit is composed of alternating dunite, harzburgite and chromitite, highly faulted, folded and metamorphosed and is cross-cut by several diabasic dykes up to few meters thick (Plate 1a).

4.2.1. Dunites

Dunite bearing outcrops occur as interlayered with harzburgites. In some places, there are dunitic lens shaped bodies of up to 500 m in diameter which may have been formed by thickening during intrafolial folding. These rocks have been strongly serpentinized and show mesh texture. They have black euhedral millimeter size disseminated chromospinels (up to 2%) with pullapart cracks and small olivine inclusions. Deformed olivines in dunites indicate mechanical twinning and lobate margins (Plate 1b). Table 1 shows modal composition and major textures of main Soghan rocks.

4.2.2. Chromitites

Chromitites in this unit are seen as two different ore deposits. The first consists of several meters size lens shaped, are found in serpentinized dunites. The second type occur as massive discontinuous layers up to 3 m thick (Plate 1d). All of the chromitites are associated with dunite and have almost similar orientation (N 70/80 SE). Layers are often cut and displaced by faults and very rich in chromite at deeper levels. Chromitites have a variety of textures (leopard, granular, massive,...) and contain euhedral chromospinels and interstitial serpentinized olivine.

4.2.3. Harzburgites

These medium to coarse grained rocks have been made the main part of the unit. In many places, these rocks are much richer in orthopyroxene (up to 40%) in volume. Orthopyroxenes exhibit two different shapes. The first generation is coarse grained and highly deformed, lying parallel to the foliation. They show kinking, flattening and contain exsolution lamellae of clinopyroxene. The second groups are fine grained, nondeformed with a higher birefringence, without exsolution lamellae and appear as interstitial phases (Plate 1c).

Fine-grained euhedral to subhedral chromospinels in

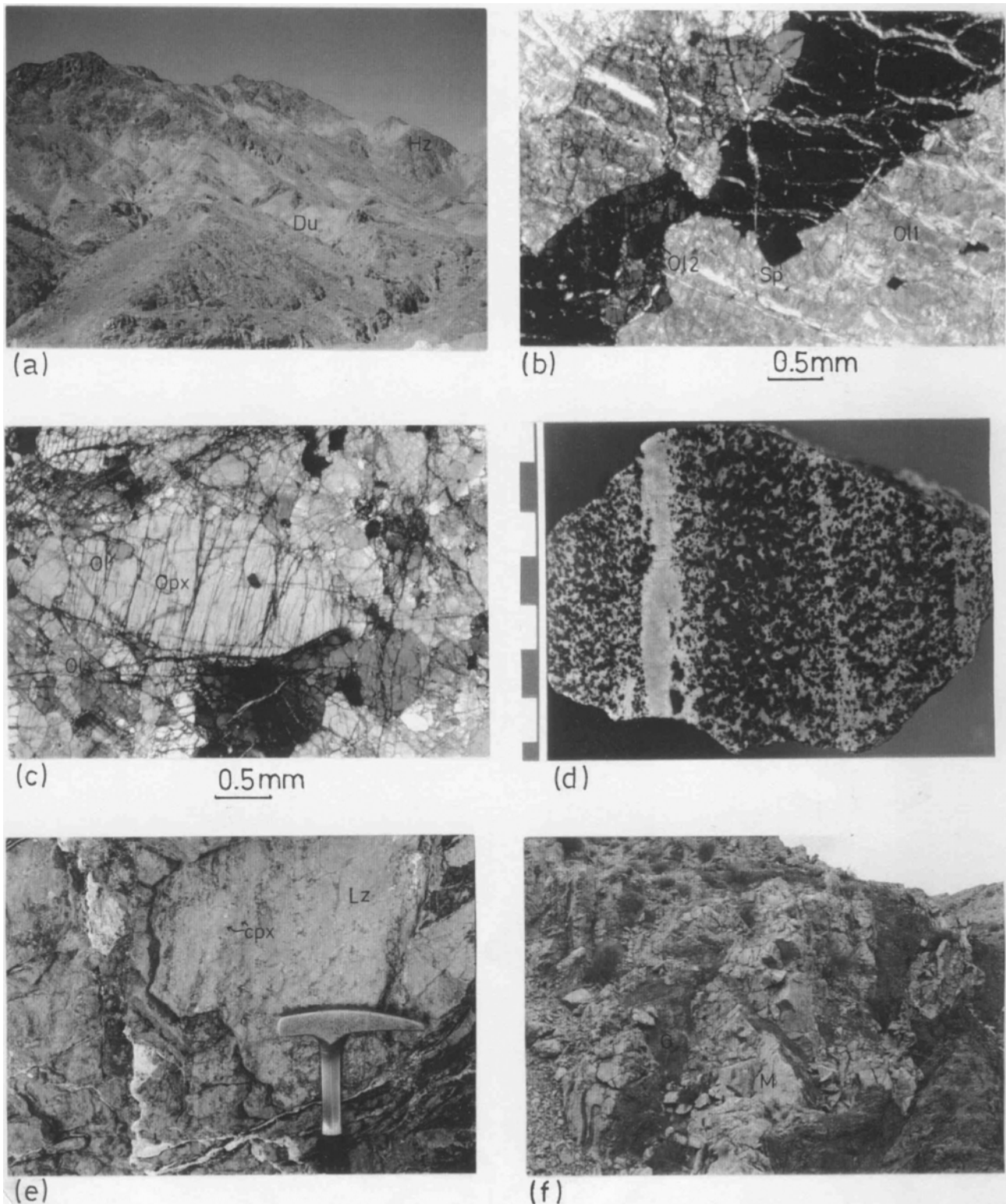


Plate 1. **a)** Alternating of dunites (Du) and harsburgites (Hz) in lower part of Soghan massif. **b)** Recrystallization of olivine (Ol) in Soghan dunite in X.P.I. image. **c)** Harsburgite's texture with a big orthopyroxene (Opx) between deformed olivines (Ol) in X.P.I. **d)** Banded chromitites in Soghan massif. **e)** Soghan lherzolites (Lz) with thin layers of clinopyroxenite (Cpx). **f)** Invasion of isotropic gabbro (G) in the Sargaz-Abshur marbles (M).

Table 1. Modal composition, texture and normative composition of Soghan rock units

Rock unit	Modal composition Vol (%)	Texture	Normative composition Mol (%)
Dunite	Ol(98), Chr(2)	Granular (medium-coarse grain)	Ol(96), Hyp(0.9), Chr(1.05), Mt(0.49)
Harzburgite	Ol(73), Opx(25), Chr(2)	Granular, Coarse grain (up to 5 mm)	Ol(74.8), Hyp(21.2), Di(0.44), An(0.79), Mt(2.16), Chr(0.33)
Lherzolite	Ol(70), Opx(18), Cpx(10), Sp(2)	Granular, Medium grain (upto 2 mm)	Ol(58.2), Hyp(23.7), Di(4), An(3.6), Mt(8.8), Chr(0.85)
Wehrlite	Ol(60), Opx(4), Cpx(35), Sp(1)	Poikilitic	Ol(32.4), Hyp(32.37), Di(34.5), An(3.8), Mt(0.3)
Cpx-Plg Gabbro	Cpx(47), Plg(50), Ti-Fe oxides(1-3)	Ad-Meso Cumulate	Ol(12.4), Hyp(13.9), Di(34.5), An(21.6), Mt(0.3), Q(6.9)
Plg-peridotite	Ol(60), Cpx(30), Plg(10)	Meso Cumulate	Ol(40.9), Hyp(10.4), Di(17), An(22.6), Mt(4.39), Ab(3.8)
Gabbro-Norite	Plg(50), Cpx(30), Opx(15), Amph(3), Sulfide and Oxides(0.5)	Equigranular-Mosaic	Ol(13.6), Hyp(12.6), Di(23.9), An(23.3), Ab(21.7)
Isotropic Gabbro	Plg(50), Cpx(47), Amph(10)	Ophitic	Ol(0.8), Hyp(1.5), Di(46.6), An(32), Ab(8.2), Or(0.9), Mt(8.6)
Ultramafic sills	Ol(55), Opx(27), Cpx(13), Sp(1), Amph(10)	Poikilitic and Mosaic	Ol(43), Hyp(30.7), Di(5), Mt(16.5), An(6.2)

Abbr.: Ol: Olivine, Opx: Orthopyroxene, Cpx: Clinopyroxene, Hyp: Hyperstene, Chr: Chromspinel, Amph: Amphibole, Plg: Plagioclase, An: Anorthite, Mt: Magnetite, Or: Orthoclase, Ab: Albite, Di: Diopside, Q: Quartz

harzburgite have a brownish colour. They occur as inclusions in olivine orthopyroxene. These phases pullapart cracks and are rarely elongated parallel to the foliation. In rare cases they contain small nondeformed olivine inclusions. Olivine crystals of up to 5 mm in size are strongly deformed with mechanical twinning, elongated and exhibit lobated grain boundaries and fine subgrains. They have been recrystallized to various degrees and include small nondeformed olivines with triple junction, which due to annealing [18,31].

In the southeastern part of the unit, just after the Soghan fault, these ultramafic rocks show petrographic differences. In this part, more than 90% vol. of olivines are strongly deformed with mechanical twinning and intense crystal elongation. Orthopyroxenes are two types but the nondeformed ones contain small dark euhedral chromspinel arranged parallel to the cleavages. In the same area, chromspinel are completely different and occur as black small euhedral crystals without any cracks.

The foliation of harzburgites is defined and developed by orthopyroxene and is distinguished from that of regional metamorphic foliation by the presence

of kinking, twinning and elongation of orthopyroxene.

4.3. Transition Zone

This unit is observed to the south-east of the previous peridotites with different thickness ranging from 50 to 600 m and marked by yellowish color and well bedded lherzolite, dunite, pyroxenite and wehrlite.

4.3.1. Lherzolites

These fresh rocks have a granular texture with highly deformed medium size olivines with lobate borders, mechanical twinning and grain boundary migration. They recrystallized to small nondeformed olivines. Orthopyroxenes have two shapes, deformed and nondeformed.

Poikilitic clinopyroxenes are often associated with orthopyroxene and olivine. Some of them show exsolution lamellae and kinkbands. In terms of deformation, they are similar to those of orthopyroxenes. Spinel in these rocks is clearly interstitial, anhedral and greenish brown in color and seems to be the last crystallized phase.

4.3.2. *Dunites*

These highly serpentinized rocks are interlayered with lherzolites. They are different from previous dunites in having 1-2% orthopyroxene and chromspinel as either isolated euhedral or completely interstitial anhedral crystals.

4.3.3. *Pyroxenites*

These rocks can be seen as layers up to 1 m thick, coarse grained, without any mineral preferred orientation and include orthopyroxenite, websterite and clinopyroxenite.

These lithologies are invaded by isotropic gabbro, by which the original clinopyroxene crystals without any preferred orientation have been recrystallized, due to metasomatic reactions between pyroxenites and the gabbro.

4.3.4. *Wehrlites*

In the upper part of this unit, the modal orthopyroxene is decreased and wehrlites are formed. They are similar to lherzolites, but large poikilitic deformed isolated clinopyroxenes are increased in these rocks.

4.4. *Layered Gabbros*

This tectonized unit crops out in the south-east of Soghan complex and includes Plg-peridotite, Cpx-Plg gabbros, norite and ferrogabbro.

4.4.1. *Cpx-Plg gabbros*

In the field, these rocks form fine-grained rocks with mafic-felsic layering up to 20 cm in thickness, trending in 90/90. In some places they show a coarse-grained texture due to the isotropic gabbro invasion.

4.4.2. *Plg-peridotites*

These altered rocks are brown in color, relatively coarse grained. They occur as enclaves of up to 5 m in diameters with a mesocumulate texture in which olivine is cumulus and clinopyroxene together with plagioclase are intercumulus. Medium-grained olivines are partly altered to serpentine with mesh texture. Around olivine crystals there is an amphibole-spinel corona texture, probably has made by olivine-melt reactions. In places, irregular radiating cracks have been formed around olivines and penetrated into the surrounding plagioclases

4.4.3. *Noritic ferrogabbros*

These fine grained rocks contain up to 0.5% vol. sulfides and iron-titanium oxides with adcumulate

texture. Stratigraphically, the modal content of the opaque minerals increases from lower to upper part. They have equigranular mosaic texture. Sulfides and iron-titanium oxides are intercumulus and must be the last phases which have been crystallized due to immiscibility. In the top of noritic ferrogabbros there is a very small outcrop of plagiogranite.

4.5. *Isotropic Gabbro*

This gabbro has cross-cut previous units and raised up into the marbles (Plate 1f) with fine to coarse-grained ophitic texture. There are several shear zones in the gabbro and the presence of secondary oriented amphiboles after clinopyroxene in shear zones, indicates that the gabbro is syntectonic and metamorphosed up to epidote-amphibolite facies.

In the upper parts of Soghan complex, isotropic gabbro is placed in the vicinity of marbles and amphibolites of Sargaz-Abshur complexes. Amphibolites have been partially molten by the isotropic gabbro and a felsic mobilizate of dioritic composition has been formed.

4.6. *Ultramafic Sills or Lavas*

In the top of layered gabbros, just below the marbles and interlayered with them, in some places there are black ultramafic-mafic rocks as layers up to 20 m thick, sheared, metamorphosed and amphibolitized. Layers internally change in modal composition and color. In some places, they have a foliation plane parallel to the shear zones (N60/90) and a lot of amphiboles have been formed. In ultramafic part they show a mosaic texture with a modal composition of wehrlitic, lherzolic or feldspathic peridotite, metamorphosed up to amphibolite facies.

4.7. *Diabasic Dykes*

These intrusions include of up to 2 m thick that have invaded all of the units. In Soghan main peridotites, the main population of dykes is concentrated in the southeastern part. They exhibit quenched margins and intruded parallel to the peridotite compositional layering (N60/80SE) having a fine grained and doleritic texture.

5. *Age Determination*

K-Ar age dating was performed on 4 amphibole mineral separates and 2 diabasic dykes in Soghan complex. Intrusion of the isotropic gabbro within Sargaz-Abshur amphibolites caused partial melting of

the amphibolites, and formed an amphibole bearing mobilizate of dioritic composition. We suggest that the age dating of the amphiboles from the mobilizate, could indicate the age of emplacement of the isotropic gabbro.

The results of K-Ar age dating of the amphiboles indicate an age range of 182+14 m.a. to 186+20 m.a. (Lower Jurassic, Toarcian). Field evidences indicate that the isotropic gabbro was intruded when Soghan complex had been completely crystallized. Therefore, the emplacement age of Soghan complex (peridotites and layered gabbros) was probably Paleozoic. K-Ar age dating of diabasic dykes indicates an age of 76+4.5 m.a. of Cretaceous time.

6. Mineral Chemistry

The results of mineral chemistry for olivine, spinel, orthopyroxene, clinopyroxene and plagioclase are shown and described as the following (Tables 2 and 3).

Table 2. a) Chemical composition of Soghan olivines, average from 195 analyses. b) Chemical composition of Soghan chromspinel, Average from 210 analyses

a)					
Lithology	Du	HZ	Lz	Webs	Plg-perid
SiO ₂	42.24	42.47	40.86	40.84	37.87
TiO ₂	0.04	-	0.01	0.10	-
Al ₂ O ₃	-	0.47	-	0.08	0.14
FeO	6.23	8.20	10.20	10.69	22.40
MnO	0.16	0.09	0.09	0.31	0.25
MgO	51.79	50.01	48.33	48.01	39.14
CaO	0.01	0.03	-	0.02	0.12
Na ₂ O	0.01	0.04	0.03	-	0.02
K ₂ O	-	-	0.01	-	-
Cr ₂ O ₃	-	0.03	0.03	0.15	0.01
NiO	0.37	0.36	0.39	0.58	0.09
Total	100.85	101.27	99.89	100.76	100.04
Si	1.01	1.02	1.01	1.00	0.98
Ti	0.00	-	0.00	0.00	-
Al IV	-	0.00	0.00	0.01	0.01
Fe ³⁺	-	-	-	-	0.03
Fe ²⁺	0.13	0.18	0.21	0.22	0.46
Mn	0.00	0.00	0.00	0.01	0.01
Mg	1.85	1.79	1.77	1.75	1.51
Ca	0.00	0.00	-	0.00	0.00
Na	0.00	0.00	0.00	-	0.00
K	-	-	0.00	-	-
Cr	-	0.00	0.00	0.00	0.00
Ni	0.01	0.01	0.01	0.01	0.00
Sum	3.00	3.00	3.00	3.00	3.00
Fa	0.06	0.08	0.11	0.11	0.24
Fo	93.68	91.57	89.41	88.89	75.70

b)

Lithology	Du	l.Hz	u.Hz	Lz	Webs	Chrt
SiO ₂	0.03	0.39	0.04	-	-	-
TiO ₂	0.10	0.05	0.06	0.06	0.19	0.04
Al ₂ O ₃	20.71	24.67	9.10	53.61	39.77	9.24
FeO	20.54	16.06	23.00	15.25	19.19	14.37
MnO	0.22	0.25	0.22	0.08	0.26	-
MgO	11.03	12.31	11.65	17.99	14.51	13.43
CaO	-	0.23	0.17	-	0.01	-
Cr ₂ O ₃	44.95	44.38	55.00	12.15	26.15	60.83
NiO	0.04	0.07	0.07	0.32	0.04	0.12
Total	97.63	96.47	99.31	99.49	100.18	98.07
Si	-	0.10	0.01	0.01	0.02	-
Ti	0.02	0.01	0.01	0.01	0.01	0.01
Al IV	6.26	7.20	2.82	12.23	5.22	2.88
Fe ³⁺	0.58	-	0.20	0.15	0.86	0.45
Fe ²⁺	3.76	3.33	4.82	2.63	4.85	2.71
Mn	0.05	0.05	4.45	0.06	0.04	-
Mg	4.21	4.54	4.27	5.31	3.11	5.27
Ca	-	0.06	0.05	0.00	0.02	-
Cr	9.11	8.69	11.70	3.58	9.85	12.66
Ni	0.01	0.02	0.01	0.02	0.02	0.02
Sum	24.00	24.00	24.00	24.00	24.00	24.00
Cr#	0.59	0.55	0.80	0.23	0.65	0.82
Mg#	0.49	0.58	0.46	0.66	0.35	0.62
FeO w%	17.54	16.06	19.64	14.42	21.89	12.33
Fe ₂ O ₃ w%	3.00	-	3.36	0.93	4.33	2.27

Abbr.: Du: Dunite, Hz: Harzburgite, Lz: Lherzolite, Webs: Websterite, Chrt: Chromitite, l.Hz: lowerHz, u.Hz: upper Hz.

6.1. Olivine

The average forsterite content of olivine in dunites, harzburgites, lherzolites, and wehrlites are 93.68, 91.57, 89.41, 80.7 mole% respectively. There is no significant variation on the olivine chemistry in Mg and Si in the dunites and harzburgites. However, the NiO average content in lower peridotites is 0.37% and decreases from dunites to plg-peridotites to the lower limit of 0.09%. Petrographically, there are two types of olivine, deformed and nondeformed in dunite and harzburgites. The MgO and SiO₂ contents are the same in both types, but in deformed ones, NiO content is higher. They lack compositional zoning.

6.2. Chromspinel

Chemically, there are 4 types of chromspinel in the Soghan complex (Table 2b):

– The composition of disseminated chromspinel in lower peridotites (northwest of Soghan fault) includes ave. 44 w% Cr₂O₃, 24.7 w% Al₂O₃, and 16 w% FeO. As illustrated in Figure 2 [12,36] they plot in the field of abyssal residual spinel peridotites. This spinel doesn't have any compositional zoning.

– The composition of disseminated chromspinel in Upper peridotites (southeast of Soghan fault) includes higher contents of Cr₂O₃ (55 w%) and FeO (23 w%) and lower content of Al₂O₃ (9.1 w%) than previous ones. They plot in the field of reaction chromites in Figure 2 [36], implies their compositions have changed by percolating melts and/or completely have crystallized from those melts.

Table 3. a) Chemical composition of Soghan orthopyroxenes, average from 165 analyses. b) Chemical composition of Soghan clinopyroxenes, average from 150 analyses

a)					
Lithology	Hz	Lz	Opxt	Webs	Fer.gab
SiO ₂	56.63	55.01	56.00	56.58	53.40
TiO ₂	0.03	0.06	0.05	0.02	0.14
Al ₂ O ₃	2.04	3.44	1.22	1.41	1.58
FeO	5.43	7.33	6.09	6.74	20.69
MnO	0.16	0.16	0.15	0.19	0.54
MgO	33.55	33.45	30.18	33.43	23.55
CaO	0.60	0.53	6.03	0.49	0.64
Na ₂ O	0.13	-	0.05	0.00	-
K ₂ O	0.07	0.02	0.01	-	-
Cr ₂ O ₃	0.58	0.57	0.47	0.40	0.02
NiO	0.16	0.04	0.07	0.03	0.06
Total	99.37	100.60	100.30	99.30	100.60
Si	1.96	1.89	1.95	1.97	1.96
Ti	0.00	0.00	0.00	0.00	0.00
Al IV	0.04	0.11	0.05	0.03	0.04
Al VI	0.05	0.03	0.00	0.03	0.03
Fe ³⁺	-	0.06	0.03	-	0.00
Fe ²⁺	0.16	0.16	0.15	0.20	0.63
Mn	0.00	0.00	0.00	0.01	0.02
Mg	1.74	1.71	1.57	1.73	1.29
Ca	0.02	0.02	0.24	0.02	0.03
Na	0.01	-	0.00	0.00	-
K	0.00	0.00	0.00	-	-
Cr	0.02	0.02	0.01	0.01	0.00
Ni	0.00	0.00	0.00	0.00	0.00
SUM	4.00	4.00	4.00	4.00	4.00
WO	1.16	1.00	11.42	0.95	1.29
En	90.62	88.16	79.57	88.98	66.11
Fs	8.23	10.84	9.01	10.07	32.60
Mg#	91.68	89.05	89.83	89.84	66.98

b)

Lithology	Hz	Lz	Cpxt	Weh	Fer.gab	Iso.Gab
SiO ₂	53.86	52.30	53.81	53.37	51.20	50.97
TiO ₂	-	0.18	0.17	0.21	0.45	0.33
Al ₂ O ₃	1.57	4.74	1.67	2.04	2.94	3.51
FeO	1.76	2.82	2.57	3.92	8.00	7.90
MnO	0.10	0.10	-	0.15	0.23	0.30
MgO	17.27	15.44	16.96	16.20	14.01	14.31
CaO	23.93	23.20	22.38	23.75	22.48	19.59
Na ₂ O	0.09	0.23	0.13	0.09	0.29	0.73
K ₂ O	0.01	0.01	-	0.04	-	0.11
Cr ₂ O ₃	0.76	0.78	0.74	0.22	0.02	0.46
NiO	0.09	0.02	0.28	0.02	0.00	0.06
Total	99.43	99.81	98.68	100.00	99.61	98.25
Si	1.97	1.91	1.99	1.95	1.91	1.91
Ti	-	0.00	0.00	0.01	0.01	0.01
Al IV	0.03	0.09	0.01	0.05	0.09	0.09
Al VI	0.04	0.12	0.06	0.04	0.04	0.07
Fe ³⁺	-	-	-	-	0.05	0.04
Fe ²⁺	0.05	0.09	0.08	0.12	0.20	0.21
Mn	0.00	0.00	-	0.00	0.01	0.01
Mg	0.94	0.84	0.93	0.88	0.78	0.80
Ca	0.94	0.91	0.89	0.93	0.90	0.79
Na	0.01	0.02	0.01	0.01	0.02	0.05
K	0.00	0.00	-	0.00	-	0.01
Cr	0.02	0.02	0.02	0.01	0.00	0.01
Ni	0.00	0.00	0.01	0.00	0.00	0.00
SUM	4.00	4.00	4.00	4.00	4.00	4.00
Mg#	94.60	90.72	92.17	88.07	75.76	76.34
WO	48.52	49.49	46.65	48.12	46.62	42.90
En	48.70	45.82	49.18	45.68	40.43	43.59
Fs	2.78	4.69	4.18	6.19	12.94	13.51

Abbr.: Hz: Harzburgite, Lz: Lherzolite, Opxt: Orthopyroxenite, Cpxt: Clinopyroxenite, Webs: Websterite, Weh: Wehrlite, Fer.gab: Ferrogabbro norite, Iso.Gab: Isotropic gabbro.

– According to Table 2b, the highest content average of Cr₂O₃ (60.8 w%) and the lowest content of Al₂O₃ (9.2 w%) in the Soghan chromspinel are reported in the massive chromitites. Chemically these minerals are completely different from the other types, as shown in Figure 2. These chromspinel have the highest average content of TiO₂ (0.27 w%) which implies they have been crystallized from a melt similar to that of boninitic composition [36]. In general, chemical composition and textures of Soghan chromitites are different from layered complex chromitites [32] and ophiolitic chromitites [3].

The composition of spinels in lherzolites is relatively poor in Cr₂O₃ (ave. 12.15 w%) and rich in Al₂O₃

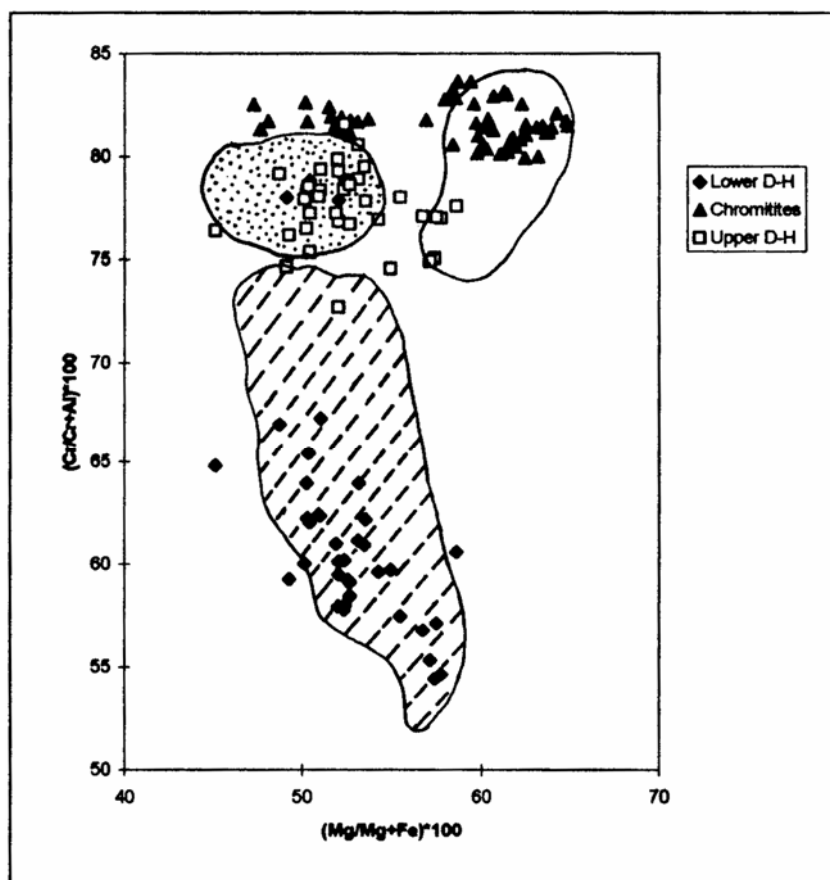


Figure 2. Comparison of Cr# vs. Mg# in Soghan chromspinel with chromspinel of Alpine peridotites (dashed area) [12], magmatic chromspinel (open area) and reaction chromspinel (dotted area) [36]. Lower D-H: Lower part of dunite harzburgites, Upper D-H: upper part of dunite harzburgites.

(53.61%), and NiO contents (0.32%) which is probably of picotite composition.

6.3. Orthopyroxene

The composition of orthopyroxene in Soghan complex is shown in Table 3a. The mole percent of En (90.62%) in both deformed and nondeformed orthopyroxenes of lower part peridotites are very similar, but the average values for TiO₂ and CaO are different in them. In highly deformed orthopyroxenes, TiO₂ and CaO in deformed orthopyroxenes are higher and NiO is lower than nondeformed ones. In the upper part of dunites-harzburgites, En content of orthopyroxenes is similar to the lower part, but Al₂O₃ content is decreased (1.2 w%), just like coexisting chromspinel. In lherzolites, the average En content of orthopyroxenes is decreased (88.16 mole%), but Al₂O₃ is increased (3.44 w%). Two types of orthopyroxenes

are also present but TiO₂ content is increased up to 0.1%. The NiO average content shows large variations, decreasing from harzburgites to pyroxenites. In noritic ferrogabbros, the average content of En is 66.1 mole%, which is close to hypersthene composition.

6.4. Clinopyroxene

This phase exists essentially in transition zone, layered gabbros and rarely in harzburgites. The average En and Cr₂O₃ content of clinopyroxene in harzburgites is higher than those of other rocks and is close to chromodiopside (Table 3b). The TiO₂ and Cr₂O₃ values of deformed clinopyroxenes in lherzolites are lower than those of nondeformed ones. Therefore, it is probable that the nondeformed clinopyroxenes have been crystallized from a melt rich in Ti, Cr and Al. The clinopyroxenes in wehrlites show compositional zoning in which Ti, Cr, Al and Ni increased from center to the

margins. According to Table 3b, the contents of Cr₂O₃ decrease in clinopyroxene from harzburgites to gabbros.

6.5. Plagioclase

The average plagioclase composition in the Plg-peridotites is 92.81 An%, which is higher than those of Plg-Cpx gabbros and isotropic gabbro.

6.6. Geothermometry

Geothermometric estimations on Soghan coexisting minerals such as Ol-Sp and Opx-Cpx were based on the geothermometers reported by Bertrand and Mercier [7], Kretz [21] and Fabries [16]. The results indicate an equilibrium temperature for Ol-Sp pair in harzburgites ranging from 900-1000°C. The equilibrium temperature for Opx-Cpx ranges from 856-919°C in lherzolites and pyroxenites. The decrease in temperature in the upper units is probably related to subsolidus equilibrium temperatures.

7. Geochemistry

7.1. Major Elements

The chemical composition of ultramafic-mafic rocks of Soghan complex is shown in Table 4. The ultramafics include dunite, harzburgite, lherzolite and pyroxenite and the mafics are all types of gabbros and diabasic dykes. The first group can be divided into dunite-harzburgite and lherzolite-pyroxenite subgroups. Dunite-harzburgites are altered and have the highest mg-number ((Mg/Mg+Fe)*100) in the Soghan massif rocks. The average mg-number decreases from the north of Soghan fault to the south of that fault. In the lherzolitic subgroup mg-number ranges from 66.7 to 82.3 and SiO₂ is slightly increases (40.4-44.6 w%). However other major elements such as CaO, Na₂O and K₂O do not show significant variations. In the mafic group, mg-number varies from 48.5 to 63.6 but the average contents of CaO, Al₂O₃, TiO₂ and Na₂O are increased. Generally there is an inverse relationship between CaO, Al₂O₃, TiO₂ and Na₂O and mg-number. Figure 3 shows variation of major element oxides vs. Mg# (Mg/Mg+Fe) in Soghan main units, which indicates two different trends, probably due to alteration.

7.2. Minor Transition Elements

Ultramafic group have very high Cr abundances (459-4303 ppm), whereas mafic group is relatively poor

in Cr (261-634 ppm). Other minor transition elements display large variation, but in some instances, such as vanadium values, there is a correlation with SiO₂ w% (Fig. 3d). Ni shows a positive correlation with mg-number. The highest Ni values (2200 ppm) and lowest Sc and V concentrations (6 and 24 ppm, respectively) occur in the lowermost ultramafics. Co also shows more or less positive correlation with mg-number. In Figure 3d and e, minor transition elements plot in two different trends for ultramafics and mafics.

7.3. Rare Earth Elements (REE)

The different rock groups of Soghan complex are generally characterized by distinct REE patterns. According to Table 4 and Figures 4 and 5, ultramafics have the lowest concentration of REE. In the ultramafics, chondrite normalized REE pattern has positive slope with a high content of HREE (Table 4). In the mafic rocks, REE pattern is without any distinct upward or downward convex, similar to MORB (Fig. 5a). As shown in Figure 4 the chondrite normalized REE pattern of ultramafics is below unity which is similar to that of mantle without significant depletion of LREE. This REE pattern is possibly the result of melt-fluid reaction with solid peridotites. Large ion lithophile elements such as Rb, Sr and Ba do not show significant variations in ultramafics, but are enriched in mafics.

In Figure 6 Soghan peridotites have been compared with other mantle peridotites [24] and the results indicate that Soghan peridotites are more depleted than other peridotites. Comparison of vanadium contents in Soghan peridotites with other mantle peridotites [8] shows that Soghan peridotites likely belong to continental mantle peridotites (Fig. 7).

8. General Discussion and Conclusions

The Soghan complex is composed of five main units: The Gachin unit (includes serpentized dunite, harzburgite and chromitite), the main Soghan unit (includes alternative dunite, harzburgite and chromitite), the transition zone (includes layered dunite, lherzolite, pyroxenites and wehrlite) and layered gabbros that overly by Sargaz-Abshur metamorphic complexes. All of these units have been invaded by an isotropic gabbro. Lowermost part of Soghan complex includes dunites and harzburgites with a weak network fabric marked by elongation and kinking in orthopyroxene and formation of small olivine crystals around large ones. These features show a high temperature-pressure mantle deformation and have been described for mantlic diapirs in some terrains [9-11]. There is not any typical

Table 4. Chemical composition of Soghan rock units (major, trace and rare earth elements), (Average from 77 analyses)

Lithology	Du	Hs	Lz	Opxt	Webs	Cpxt	Weh	Plg-perid	Cpx-plgGab	Fer.gab	Iso.Gab	Plagiogr	Diab.dyke	Ul.sill
SiO ₂	40.90	42.00	44.60	55.00	51.00	50.30	40.40	42.00	48.30	48.30	47.30	73.30	49.70	38.80
TiO ₂	0.02	0.02	0.06	0.05	0.06	0.20	0.07	0.13	0.24	0.42	0.37	0.27	0.55	0.81
Al ₂ O ₃	0.06	0.59	2.40	1.40	1.30	4.10	2.20	11.45	12.30	13.50	15.50	12.74	16.10	3.70
Fe ₂ O ₃	8.60	7.00	8.80	7.30	5.30	6.30	14.50	10.65	9.00	11.00	5.70	3.54	10.02	13.90
MnO	0.12	0.10	0.13	0.16	0.13	0.15	0.17	0.15	0.17	0.24	0.10	0.07	0.18	0.15
MgO	42.72	42.50	40.89	32.68	22.35	17.67	29.09	18.60	11.40	10.34	8.59	1.65	5.90	31.46
CaO	0.76	0.40	2.60	2.95	15.51	20.29	4.61	10.15	14.38	13.96	18.49	2.48	10.31	2.38
Na ₂ O	0.05	0.06	0.03	0.03	0.10	0.13	0.06	0.54	1.03	0.63	1.08	2.70	4.34	0.11
K ₂ O	0.16	0.02	0.14	0.11	0.07	0.06	0.13	0.06	0.15	0.04	0.19	0.12	0.30	0.13
P ₂ O ₅	0.01	-	0.01	0.02	0.01	0.01	-	0.02	0.02	0.01	-	0.03	0.07	0.07
L.O.I.	6.32	6.84	0.83	0.59	3.19	1.56	9.09	5.44	2.57	0.57	2.16	2.87	2.21	9.27
Total	100.23	99.53	100.43	100.25	99.08	100.79	100.28	99.19	99.62	99.06	99.42	99.77	99.68	100.75
Traces ppm														
Rb	0.38	0.50	0.59	0.62	0.22	0.22	0.26	1.70	1.41	0.23	2.39	1.20	8.00	0.52
Sr	4.00	1.00	1.00	5.00	12.00	12.00	14.00	115.00	112.00	119.00	345.00	150.00	127.00	38.00
Ba	2.00	1.00	2.00	9.00	13.00	10.00	20.00	40.00	28.00	11.00	156.00	78.00	49.00	44.00
Sc	8.70	6.00	15.40	21.00	39.60	88.80	28.80	51.00	72.70	71.80	55.50	8.80	35.00	15.70
V	39.00	24.00	75.00	70.00	117.00	277.00	93.00	105.00	273.00	295.00	237.00	25.00	250.00	122.00
Cr	2,293.00	2,000.00	2,740.00	4,303.00	3,050.00	1,453.00	459.00	325.00	634.00	261.00	334.00	124.00	100.00	2,376.00
Co	98.00	100.00	91.00	56.00	38.00	34.00	127.00	81.00	37.00	39.00	35.00	4.00	35.00	126.00
Ni	2,150.00	2,200.00	1,913.00	555.00	490.00	126.00	304.00	150.00	55.00	56.00	127.00	6.00	18.00	1,712.00
Y	0.70	0.20	1.90	0.90	2.20	4.30	1.20	3.50	4.30	8.90	7.51	4.70	14.90	7.40
Zr	6.00	2.00	4.00	4.00	2.00	5.00	6.00	6.00	5.00	7.00	11.00	-	36.00	63.00
Nb	-	0.20	1.01	0.20	0.06	0.08	0.11	0.25	0.28	0.16	0.19	0.65	2.70	6.93
La	0.00	0.10	0.49	0.27	0.11	0.33	0.22	0.45	0.42	0.51	1.23	3.20	3.40	4.90
Ce	0.02	1.00	0.81	0.47	0.29	0.75	0.48	2.00	0.90	1.43	2.91	6.50	7.20	11.40
Pr	0.00	-	0.10	0.05	0.06	0.12	0.06	-	0.14	0.28	0.41	-	-	1.56
Nd	0.02	-	0.44	0.25	0.38	0.71	0.29	0.40	0.79	1.70	2.32	3.40	4.40	7.20
Sm	0.01	-	0.16	0.07	0.14	0.32	0.09	0.15	0.35	0.78	0.89	0.80	44.00	1.67
Eu	0.00	0.04	0.05	0.01	0.05	0.11	0.03	0.24	0.17	0.34	0.34	0.95	0.52	0.53
Gd	-	-	0.15	0.03	0.17	-	0.11	-	0.45	1.01	1.06	0.80	2.00	1.60
Tb	-	-	0.04	0.02	0.04	-	0.02	-	0.10	0.23	0.22	-	-	0.26
Dy	0.03	-	0.29	0.12	0.33	0.03	0.18	0.55	0.75	1.56	1.42	0.80	2.50	1.56
Ho	0.01	-	0.08	0.03	0.07	0.01	0.05	-	0.18	0.38	0.32	-	-	0.31
Er	0.02	-	0.23	0.11	0.20	0.02	0.14	0.35	0.49	0.99	0.81	0.50	1.50	0.73
Tm	0.00	-	0.04	0.02	0.03	0.00	0.02	-	0.07	0.14	0.12	-	-	0.10
Yb	0.04	0.02	0.24	0.12	0.20	0.04	0.14	0.32	0.44	0.91	0.70	0.50	1.58	0.60
Lu	0.01	-	0.04	0.02	0.03	0.01	0.02	-	0.07	0.14	0.11	-	-	0.08
Hf	0.01	-	0.10	0.02	0.03	0.01	0.04	-	0.09	0.16	0.49	-	-	1.87
Ta	-	-	0.02	0.01	0.00	-	0.01	-	0.01	0.01	0.02	-	-	0.59
W	1.09	-	-	-	-	-	37.02	-	-	-	1.50	-	-	-
Pb	-	-	2.29	2.18	6.33	1.09	0.84	-	3.45	1.03	0.87	-	-	1.02
Th	0.01	-	0.21	0.08	0.07	0.01	0.06	0.20	0.14	0.10	0.16	0.25	0.85	0.70
U	0.01	-	0.44	0.05	0.08	0.01	0.10	-	0.44	0.09	0.13	-	-	0.29
Mg#	83.24	85.86	82.29	81.74	80.83	73.72	66.74	63.59	55.88	48.45	60.11	31.30	37.06	69.36

Abbr.: Du: Dunite, Hs: Harzburgite, Lz: Lherzolite, Opxt: Orthopyroxenite, Cpxt: Clinopyroxenite, Webs: Websterite, Weh: Wehrlite, Cpx-plg-gab: Cpx-Plg gabbro, Fer.gab: Ferrogabbro, Iso.gab: Isotropic gabbro, Plagiogr: Plagiogranite, Diab.dyke: Diabasic dykes, Ul.sill: Ultramafic sills

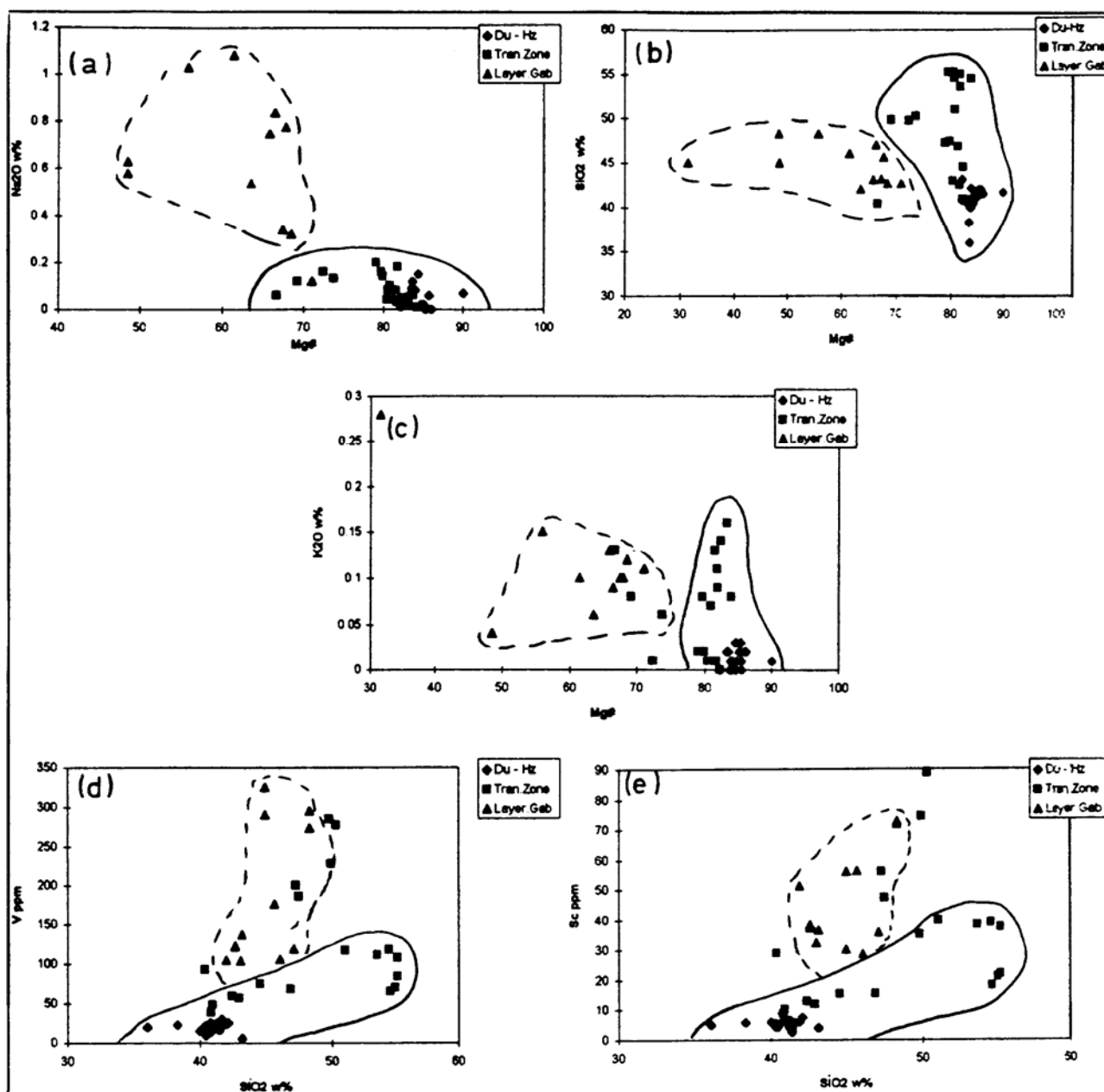


Figure 3. Variation diagrams for Soghan rock units. Du: Dunite, Hz: Harzburgite.

tectonite ophiolitic texture [34,26] in them, indicating that the Soghan complex is probably a part of a mantle diapir. In addition, these features show that the Soghan complex is not a typical defined traditional ophiolitic assemblage. Chemically, disseminated chromspinel plot in residual peridotites [12]. Geochemical studies reveal that chemical composition of Soghan harzburgites is very similar to depleted mantle peridotites [25]. They have been more than 20% partially melted. This degree of partial melting has

calculated by current distribution coefficients [15,18]. Several authors have been assumed that these types of harzburgites are residual rocks that have been formed by partial melting of garnet or spinel lherzolite [6,13,5,17,14]. In addition, chondrite normalized REE patterns for these rocks are lower than unity, similar to mantlic rocks, without depletion of LREE. This profile is likely formed by interaction and refertilization of these peridotites due to percolating melts.

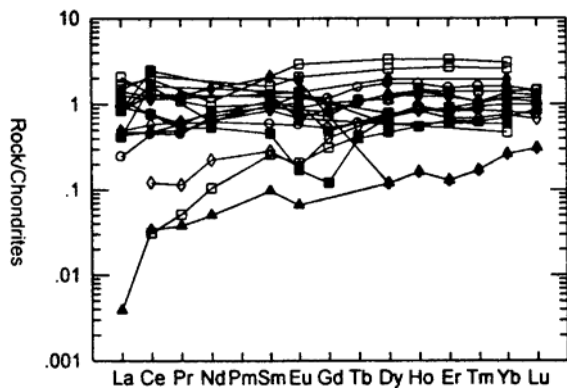


Figure 4. Chondrite normalized rare earth elements patterns of Soghan ultramafic and mafic units. (▲) Dunites, (■) clinopyroxenites, (◇) orthopyroxenites, (□) lherzolites, (◆) wehrlites [1].

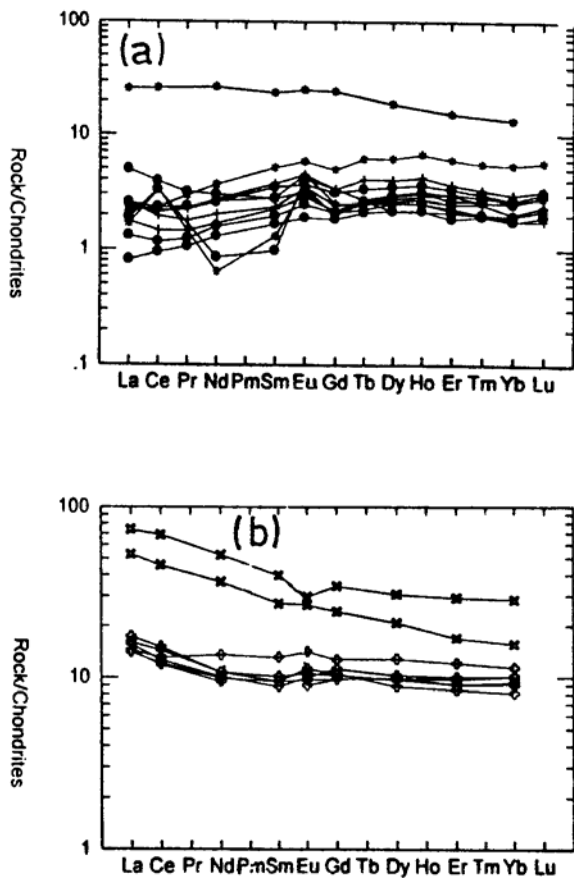


Figure 5. Chondrite normalized rare earth patterns of Soghan mafic rocks. a) Layered gabbros, (*) Cpx-Plg gabbros, (+) Norites, (●) Feldspathic peridotites. b) (+) diabasic dykes, (x) Pillow lavas in northern coloured melange.

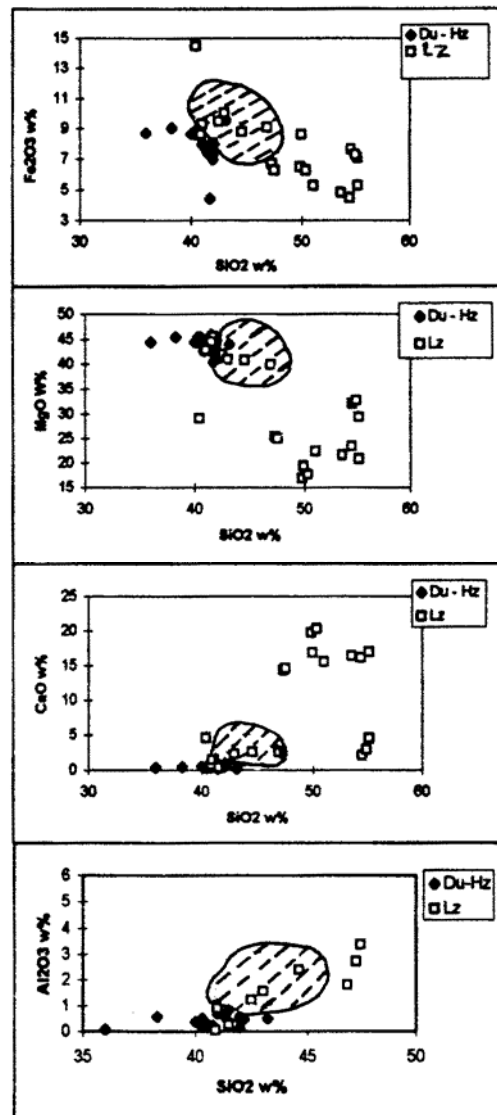


Figure 6. Variation of major elements oxides vs. SiO₂ in Soghan peridotites and comparison with other mantle peridotites (dashed area), [24]. Soghan harzburgites have lower content of Al₂O₃, CaO, and FeO then other mantle peridotites. Du: Dunite, Hz: Harzburgite, Lz: Lherzolite.

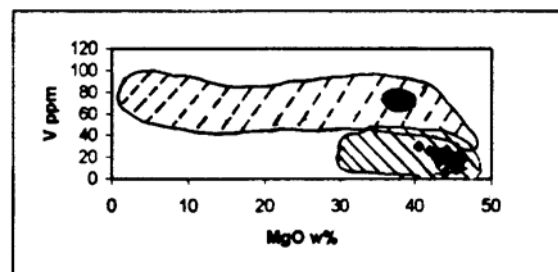


Figure 7. Variation of vanadium content (ppm) vs. MgO w% in primitive mantle (black area), oceanic peridotites (dashed area), cratonic peridotites (shaded area), [8] and Soghan peridotites (◆).

Percolation and impregnation processes have been reported in many ultramafic and mantlic associations [4,35,28,20]. There are several evidences indicating percolation processes in Soghan complex. In some parts of the harzburgites, there is one type of orthopyroxene with no deformation and exsolution texture and is completely interstitial. So, it can be either completely crystallized from an ascending melt or possibly percolating melts have dissolved former clinopyroxene-orthopyroxene and formed this new generation of orthopyroxene [19].

In the south-east of Soghan fault, percolation of a pervasive melt marked by existence of small euhedral black chromspinel enriched in Cr and poor in Al and completely different from others. In the Cr-number $((Cr/Cr+Al)*100)$ vs. Mg-number $((Mg/Mg+Fe)*100)$ diagram they form a separated field similar to reaction chromspinel which considered by Zhou *et al.* [36]. These spinels either can be formed from reaction between previous spinels with percolating melts or entirely crystallized by that melt. The latter process is more probable, because there is not any significant compositional zoning in these chromspinel. If ascending melts dissolve clinopyroxene in greater depth, it will be rich in Cr and Ca and can precipitate chromspinel and clinopyroxene in other parts [19].

There are many models for the formation of chromitites [22,23,27]. In Soghan complex, there are many chromitite mines that have been developed as discontinuous layers into the dunites. These layers are parallel to the general foliation and layering of peridotites. Soghan chromitites show magmatic features and chemically plot in boninitic chromites' field. Therefore, possibly in an ascending diapir, different steps of partial melting have been occurred. Resulting melts move upward and react with host peridotites, change their composition into boninites and crystallize chromite and olivine in nearly vertical channels. Then these chromitite bearing dunites involve in diapiric lateral movements and discontinuous parallel chromitites are formed. Leblanc [22] and Malpas *et al.* [23] have represented the same mechanism for the formation of Poum chromitites (New Caledonia).

It is conceived that following scenario may be adapted for the origin of Soghan complex. Mantle diapirism and continental thinning with concomitant underplating of mantle diapir have occurred in Paleozoic. In this stage, continental crust is thinned and lherzolitic upper mantle ascends as a diapir. The diapir is partially melted due to reducing pressure, the resulting melts produce transition zone and cumulate in the top of complex, leaving behind depleted harzburgites and dunites. At the second stage, the diapir

is partially remelted and another melts, such as ultramafic sills are formed. The magma reacts with earlier peridotite and its composition changes into boninite. The resulting melts can crystallize chromite bearing dunites. Dunites involve in diapiric lateral movement and form discontinuous and parallel layers. Then probably in early Kimmerian orogenic phase, the complex is metamorphosed. In a new vertical diapiric movement in upper Triassic lower Jurassic, an ascending melt (more probably isotropic gabbro) invades and impregnates the whole rocks and emplaces on the top of complex. Figure 8 shows these events. Therefore, Soghan complex is similar to Tinaquillo complex (in Venezuela), Ronda (in Spain) and External Ligurid peridotites (in Italy).

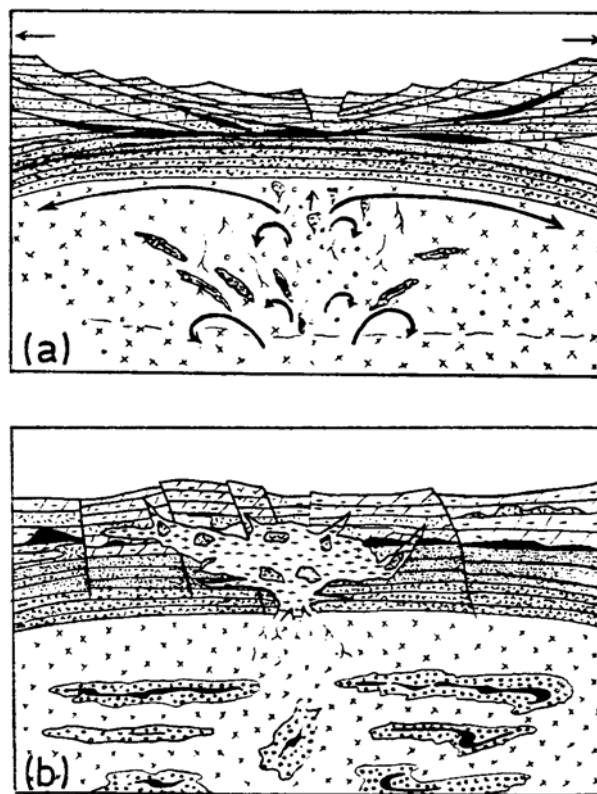


Figure 8. Mantle diapirism and evolution of Soghan complex. a) First extensional phase, ascending lherzolitic mantle diapir, crustal thinning and partial melting of the diapir. Resulting melts move upward and form transition zone and layered gabbros. In the next partial melting events, other melts such as ultramafic sills' magma are formed and react with peridotites, and crystallize chromitite-bearing dunites. b) Ascending and intrusion of isotropic gabbro into the Soghan complex and metamorphism of the complex due to early kimmerian orogenic phase. It is probable that Abdasht, Soghan and Sikhoran complex locate on different parts of the diapir.

9. Acknowledgement

The authors are grateful to Research Council of Islamic Republic of Iran for allocation of research grant for this project. We are deeply reconnaissantes to members of age dating and ICP laboratories of Louis Pasteur and Jusieu Universities in French. We enjoyed a lot of discussions which we had with Dr. T. Juteau, Dr. Aftabi and Dr. L. E. Ricou for which we express our sincere gratitude.

References

- Ahmadipour H., Sabzehei M., Whitechurch H., and Juteau T. Geological identity of Soghan ultramafic-mafic complex, south-east Iran. Scientific quarterly journal, *Geosciences, G.S.I.*, **7**(27-28): 38-53 (1999).
- Ahmadipour H. Petrology and geochemistry of Soghan and Abdasht ultramafic-mafic complexes, north-west of Dowlatabad Baft. Ph.D thesis , T.M.U. 430 p. (2000).
- Ahmed A.H., Arai S., and Attia A.K. Petrological characteristics of podiform chromitites and associated peridotites of the PanAfrican Proterozoic ophiolite complexes of Egypt. *Minerlun Deposita*, **36**: 72-84 (2001).
- Batanova N. and Sobolev A. Chemistry of mantle peridotites from Troodos ophiolites. *Ophioliti*, **24**(1a): 57-58 (1999).
- Bedini R.M., Bodinier J.L., Doutriaux J.M., and Morten L. Evolution of LILE-enriched small melt fractions in the lithospheric mantle: a case study from the East African rift. *Earth and Planetary Science Letters*, **153**: 67-83 (1997).
- Bernstein S., Kelemen P.B., and Kent Brooks C., Depleted spinel harzburgite xenoliths in tertiary dykes from East Greenland: Restites from high degree melting. *Ibid.*, **154**: 72-100 (1998).
- Bertrand P. and Mercier J.C.C. The mutual solubility of coexisting ortho and clinopyroxene: toward and absolute geothermometer for the natural system? *Ibid.*, **76**: 109-122 (1985-86).
- Canil D. Mantle redox and contrasting tectonic provenance for oceanic and cratonic mantle lithosphere, *Ophioliti*, **24**(1a): 78-79 (1999).
- Ceuleneer G., Nicolas A., and Boudier F. Mantle flow pattern at an oceanic spreading center: The Oman peridotite record. *Tectonophysics*, **151**: 1-26 (1988).
- Ceuleneer G. and Rabinowicz M. Mantle flow and melt migration beneath oceanic ridges: Models derives from observations in ophiolites. In: Mantle flow and melt generation at mid-Ocean ridges, Geophysical monograph, 71, American Geophysical Union, 123-154 (1992).
- Ceuleneer G., Monnereau M., and Amri I. Thermal Structure of a fossil mantle diapir inferred from the distribution of mafic cumulates. *Nature*, **379**: 149-153 (1996).
- Dick H.J.B. and Bullen T. Chromian spinel as a petrogenetic indicator in abyssal and alpine-type peridotites and spatially associated lavas. *Contrib. Mineral. Petrology*, **86**: 54-76 (1984).
- Eggings S.M., Rudnick R.L., and McDonough W.F., The composition of peridotites and their minerals: a laser ablation ICP-MS study. *Earth and Planetary Science Letters*, **154**: 53-71 (1998).
- Elton D., Chemical trends in abyssal peridotites: reformation of depleted suboceanic mantle. *Journal of Geophysical Research*, **97**(B6): 9015-9025 (1992).
- Elton D., Stewart M., and Ross D.K., Compositional trends of minerals in oceanic cumulates. *Ibid.*, **97**(B11): 15189-15199.
- Fabries J. Spinel-Olivine geothermometry in peridotites from ultramafic complex. *Contrib. Mineral. Petrology*, **69**: 329-336 (1979).
- Frey F.A., Suen J., and Stockman H.W. The Ronda high temperature peridotite, geochemistry and petrogenesis. *Geochemica et Cosmochemica Acta*, **49**: 2469-2491 (1985).
- Jaques A.L. and Green D.H., Anhydrous melting of peridotite at 0-15 kb pressure and the genesis of tholeiitic basalts. *Contrib. Mineral. Petrology*, **73**: 287-310 (1980).
- Kelemen P.B., Dick H.J.B., and Quick J.E. Formation of harzburgite by pervasive melt-rock reaction in the upper mantle. *Nature*, **358**: 635-641 (1992).
- Kelemen P.B., Whitehead J.A., Aharonov E., and Jordahl K.A., Experiment on flow focusing in soluble porous media, with applications to melt extraction from the mantle. *Journal of Geophysical Research*, **100**(B1): 475-496 (1995).
- Kretz R. *Metamorphic Crystallization*. John Wiley and Sons, 507 p. (1994).
- Leblanc M. Chromitite and ultramafic rock compositional zoning through a paleotransform fault, Poom, New Caledonia, a reply. *Economic Geology*, **92**: 503-504 (1998).
- Malpas J., Robinson P.T., and Zhou M.F. Chromitite and ultramafic rock compositional zoning through a paleotransform fault, Poom, New Caledonia, a discussion. *Ibid.*, **92**: 502-504 (1998).
- McDonough W.F. and Frey F.A. Rare earth elements in upper mantle rocks, In: Lipin B.R. and McKay G.A. (Eds.), *Geochemistry and mineralogy of rare earth elements*, Rev. in mineralogy. *Min. Soc. Am.*, **21**: 99-145 (1989).
- Michael P.J. and Bonatti E. Peridotite composition from the north Atlantic: regional and tectonic variation and implications for partial melting. *Earth and Planetary Science Letters*, **73**: 91-104 (1985).
- Nicolas A. *Structures of Ophiolites and Dynamics of Oceanic Lithosphere*. Kluwer Academic Press, 367 pp. (1989).
- Proenza J.A., Gervilla F., Melgarejo J.C., Vera O., Alfonso P., and Fallick A. Genesis of sulfide-rich chromite ores by the interaction between chromitite and pegmatitic olivine-norite dikes in the Potosi Mine (Moabacoa ophiolitic massif eastern Cuba). *Minerallun Deposita*, **36**: 568-669 (2001).
- Quick J.E. Petrology and petrogenesis of the Trinity peridotite, an upper mantle diapir in the eastern Klamath mountains, northern California. *Journal of Geophysical Research*, **89**(B12): 11837-11893 (1981).
- Sabzehei M. Les melange ophiolitiques de la region

- d'Esfandagheh, these d'etate, Universite scientifique et medicale de Grenoble, France, 306 p. (1974).
30. Sabzehei M., Berberian M., Alavi-Tehrani N., Houshman Zadeh A., Nougole-Sadat M.A.A., and Madjidi B. Geological quadrangle map of Iran, No. 112, Geological survey of Iran (1994).
 31. Sabzehei M. Upper protozoic-Lower paleozoic ultramafic-mafic association of south-east Iran, Product of an ophiolitic magma of komatiitic affinity. Inter. Ophiolite Symp. Finlan. Abst., 201 (1998).
 32. Spier C.A. and Filho C.F.F. The chromite deposits of the Bacuri mafic-ultramafic layered complex, Guyana shield, Amapa` state, Brazil. *Economic Geology*, **96**: 817-835 (2001).
 33. Stocklin J. Possible ancient continental margins in Iran. In: Burk C.A. and Drake C.D. (Eds.), *Geology of continental margins*, Springer, 873-887 (1974).
 34. Suhr G. Evaluation of upper mantle microstructures in the Table Mountain massif (Bay of Island). *Journal of Structural Geology*, **15**(11): 1273-1292 (1993).
 35. Vetter S.K. and Stakes D.S. Repeated magma injection and the geochemical evolution of the Northern Semail plutonic suite. In: J. Malpas *et al.* (Eds.), *Ophiolites, oceanic crustal analogues*, Pr. Symp. Troodos, Geological survey of Cyprus, 397-413 (1990).
 36. Zhou M., Robinson T., Malpas J., and Li Z. Podiform chromitites in the Loubosa ophiolite (Southern Tibet); Implications for melt-rock interaction and chromite segregation in the upper mantle. *Journal of Petrology*, **37**(1): 3-21 (1996).